Hindawi Publishing Corporation
Advances in Materials Science and Engineering
Volume 2011, Article ID 757543, 7 pages
doi:10.1155/2011/757543

Research Article

Numerical Simulation for Thermal Shock Resistance of Ultra-High Temperature Ceramics Considering the Effects of Initial Stress Field

Weiguo Li,[1] Tianbao Cheng,[1] Dingyu Li,[1] and Daining Fang[2]

[1] *Department of Engineering Mechanics, College of Resources and Environmental Science, Chongqing University, Chongqing 400030, China*
[2] *Laboratory of Turbulence and Complex Systems and College of Engineering, Peking University, Beijing 100871, China*

Correspondence should be addressed to Weiguo Li, wgli@cqu.edu.cn

Received 29 June 2011; Accepted 13 September 2011

Academic Editor: Daolun Chen

Taking the hafnium diboride ceramic as an example, the effects of heating rate, cooling rate, thermal shock initial temperature, and external constraint on the thermal shock resistance (TSR) of ultra-high temperature ceramics (UHTCs) were studied through numerical simulation in this paper. The results show that the external constraint has an approximately linear influence on the critical rupture temperature difference of UHTCs. The external constraint prepares a compressive stress field in the structure because of the predefined temperature field, and this compressive stress field relieves the tension stress in the structure when it is cooled down and then it improves the TSR of UHTCs. As the thermal shock initial temperature, a danger heating rate (or cooling rate) exists where the critical temperature difference is the lowest.

1. Introduction

Ultra-high temperature ceramics (UHTCs) offer a series of good properties including extremely high-melting point as well as chemical and physical stabilities in the ultra-high temperature environment with oxygen. They are the most potential candidates for high-temperature structural applications [1–3]. However, due to the inherent brittleness of ceramics, their poor thermal shock resistance (TSR) has been a major reason of the destruction in the thermostructural engineering for a long time [4–6]. Therefore, improving the TSR of ceramics has been one of the most important problems in the research of ceramics industry, and the highly-accurate evaluation of the TSR of ceramics is the foundation of this research.

At present, most of the theoretical theories about the TSR focus on the influence of the length and density of cracks on TSR of UHTCs [7–10]. At the same time, some new theories of evaluating the TSR have been reported continually [10, 11]. The experiments of TSR are universal, and the residual strength is used to characterize the TRS of UHTCs after quenching tests. Water, air, and liquid nitrogen are the commonly used cooling medium [4, 12–14]. Besides, electric resistance method [15] and hydrogen-oxygen torch [3] are also used to study the TSR of the UHTCs.

The material parameters of UHTCs are sensitive to temperature [2], and it is significant to take into account the temperature dependence of those parameters for the high-temperature application [11, 16]. In addition, being a part of the thermal protection system (TPS), the UHTCs must be in the affection of external constraint during the factitive period. So the TSR of UHTCs is not only the TSR of material its own, but also sensitive to the external constraint [17]. However, the existing studies are mostly focused on the TSR of material of its own; few of them take the factitive environment into account.

This paper taking the hafnium diboride (HfB_2) ceramic as an example, the effects of heating rate, cooling rate, thermal shock initial temperature, and external constraint on the TSR of UHTCs have been studied in detail. The results of this study will help to understand and evaluate the TSR of UHTCs, which used as the thermal protection material and

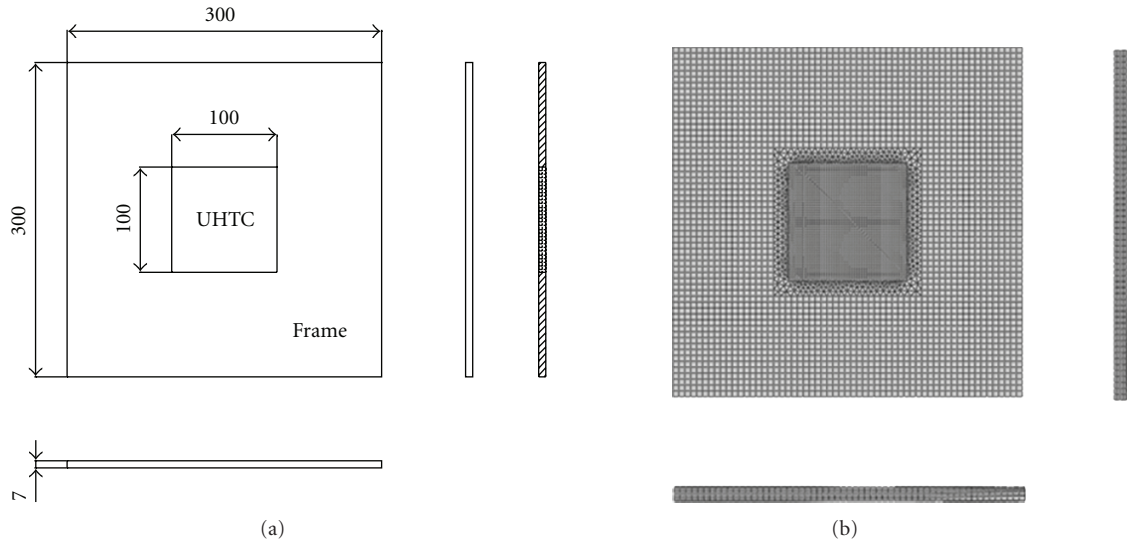

Figure 1: The orthographic views of (a) the geometric model and (b) the computational mesh.

give some helpful suggestions about improving the TSR of UHTCs.

2. The Finite Element Analysis Model

The numerical simulation for TSR of thermal protection materials was accomplished using the large general-purpose element analysis software SIMULIA Abaqus v6.9.1. The geometric model is shown in Figure 1(a) (dimensions in millimeters). And the four sides of the FRAME and its backside, including the back of the UHTC plate, are restricted by applying the symmetric constraint. The computational mesh is shown in Figure 1(b). The C3D8T element (three-dimensional, eight-node, and temperature-displacement coupled element) is used for the UHTC plate. The transition region between the UHTC plate and FRAME is C3D6 element (three-dimensional, six-node, and linear wedge element), and the rest of the FRAME is C3D8 element (three-dimensional, eight-node element).

As an example, HfB_2 ceramic is used for simulation, with material parameters [2, 18, 19] in Table 1. The relationship between the Young's modulus and temperature has been presented in [19] based on the experimental data [2],

$$E(T) = E_0 - B_0 T \exp\left(-\frac{T_m}{T}\right) + B_1[T - B_2 T_m + \mathrm{abs}(T - B_2 T_m)] \exp\left(-\frac{T_m}{T}\right). \quad (1)$$

In addition, there is no heat exchange between the FRAME and UHTC plate. The various Young's modulus of the FRAME are selected to account the restriction from the other parts of the TPS that applied on the UHTC plate. The Poisson's ratio of the FRAME is taken to be 0.3.

Assumptions that have been adopted for simulating the TSR of thermal protection materials are given below.

Table 1: Temperature-dependent material parameters of HfB_2 [2, 18, 19].

Material parameters	Values and expressions
E_0(GPa), B_0, B_1, B_2	441, 2.54, 1.9, 0.363
$k[W \cdot (m \cdot {}^\circ C)^{-1}]$	$-8.3455 \times \ln(T) + 128$
$\alpha({}^\circ C^{-1})$	$(2\ln(T) - 5) \times 10^{-6}$
$T_m({}^\circ C)$	3380
ν	0.12
$\rho(g \cdot cm^{-3})$	10.5
σ_{th}^0(MPa)	448
$C_p[kJ(kg \cdot K)^{-1}]$	$1.5328 + 1.635 \times 10^{-4} \times T - 4.8086 \times 10^4 \times T^{-2}$

(1) Both the UHTC plate and FRAME are continuous, homogeneous, and isotropic.

(2) All material parameters of the UHTC plate are functions of temperature.

(3) The connection is perfect, and there is no heat exchange between the UHTC plate and FRAME, and the temperature of the FRAME is constant being equal to the predefined temperature field 20°C.

The thermal boundary conditions are applied to the superior surface of the UHTC plate in the form of constant heating rate or cooling rate. The initial stress field is set up by slow heating from the predefined temperature field to the thermal shock initial temperature field. Here, we regard that the UHTC plate rupture once the thermal stress of the superior surface caused by thermal shock is greater than the fracture strength of the materials corresponding to the current temperature. The temperature of the superior surface is the critical rupture temperature, and the difference between the critical rupture temperature and the thermal shock initial temperature is the critical rupture temperature difference.

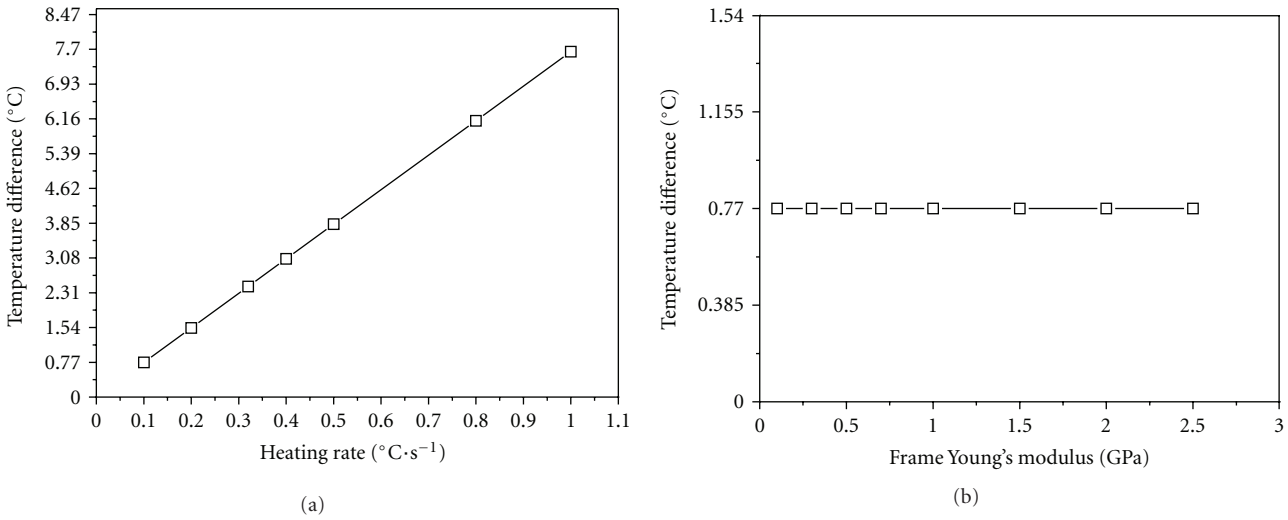

(a) (b)

Figure 2: The temperature difference between the superior surface and bottom surface of the ceramic plate versus (a) the rate of slow heating (the frame Young's modulus 1 GPa) and (b) the frame Young's modulus (slow heating rate 0.1°C·s^{-1}).

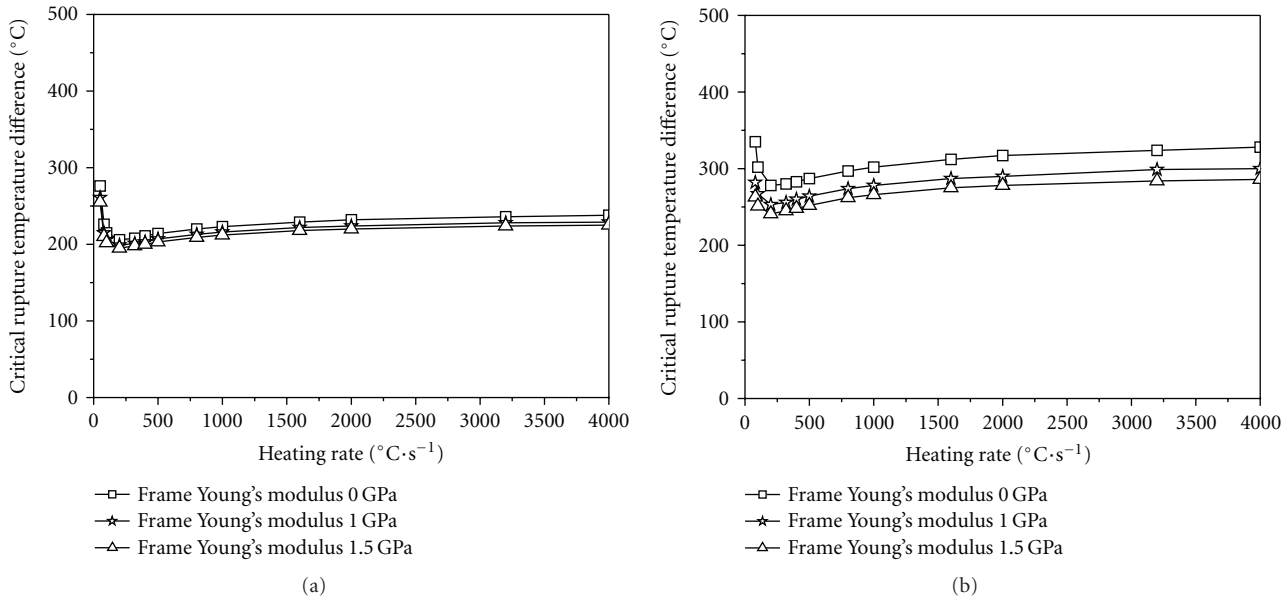

(a) (b)

Figure 3: The critical rupture temperature difference versus heating rate for different frame Young's modulus with the thermal shock initial temperature (a) 1000°C and (b) 1500°C.

The temperature-dependent fracture strength model for ultra-high temperature ceramics has been obtained in [20],

$$\sigma_{\text{th}}(T) = \sigma_{\text{th}}^{0}\left[\frac{1}{E_0}E(T)\left[1 - \frac{1}{\int_0^{T_{\text{m}}} C_{\text{p}}(T)dT}\int_0^{T} C_{\text{p}}(T)dT\right]\right]^{1/2}, \tag{2}$$

where $\sigma_{\text{th}}(T)$ is the temperature-dependent fracture strength, σ_{th}^{0} and E_0 are the strength and elastic modulus at the reference temperature, respectively, $E(T)$ is the temperature-dependent elastic modulus, T_{m} is the melting point of the material, and $C_{\text{p}}(T)$ is the specific heat at constant pressure.

3. Establishment of the Initial Stress Field

The initial stress field has been set up before thermal shock by slow heating from the predefined temperature field 20°C to the thermal shock initial temperature field. Noting that the rate of slow heating should be so small that the temperature

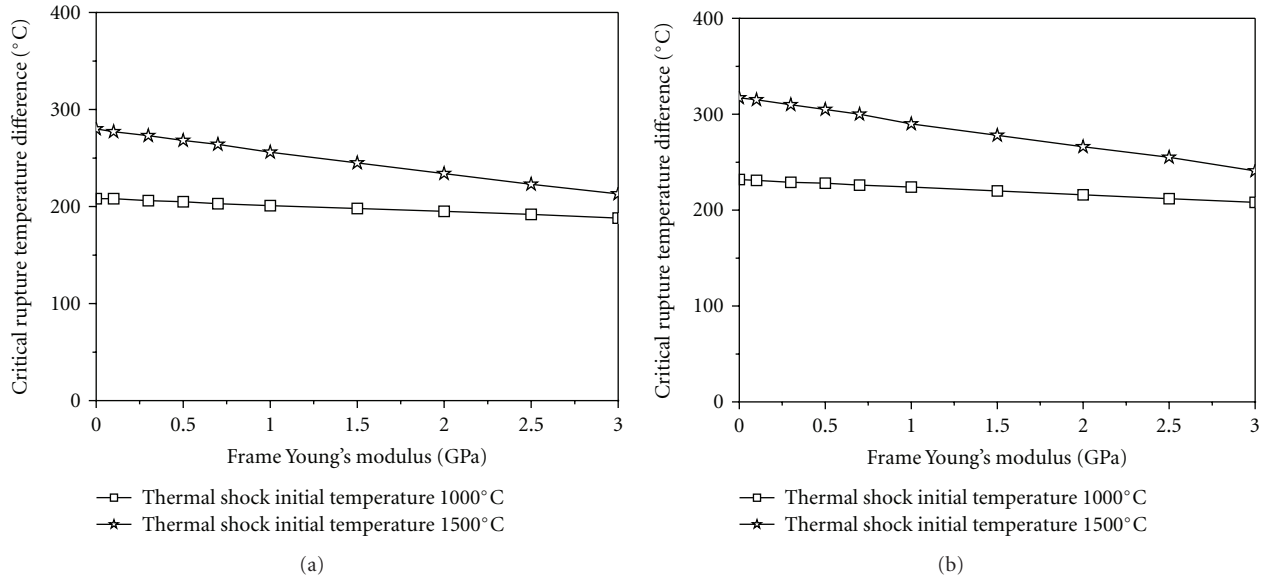

Figure 4: The critical rupture temperature difference versus frame Young's modulus for different thermal shock initial temperature with the same heating rate (a) $320°C \cdot s^{-1}$ and (b) $2000°C \cdot s^{-1}$.

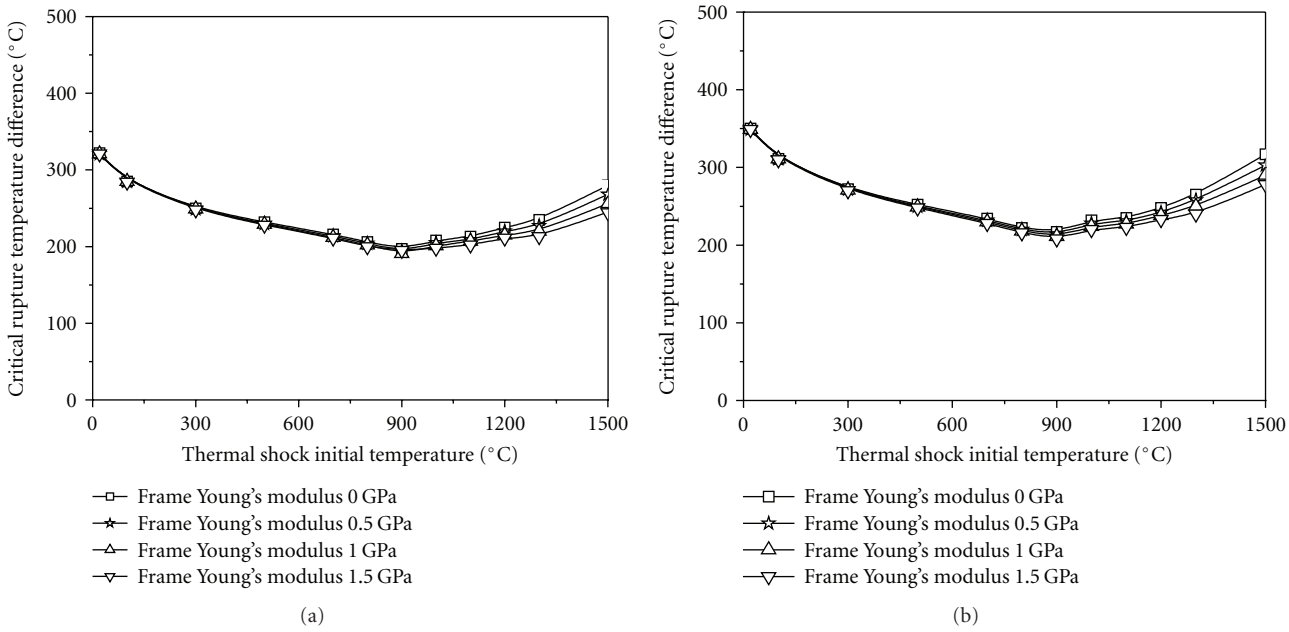

Figure 5: The critical rupture temperature difference versus thermal shock initial temperature for different frame Young's modulus with the same heating rate (a) $320°C \cdot s^{-1}$ and (b) $2000°C \cdot s^{-1}$.

difference between the superior surface and bottom surface of the ceramic plate is small enough and the initial stress field in the plate is almost even distributed.

The temperature difference between the superior surface and bottom surface of the ceramic plate corresponding to the rate of slow heating and frame Young's modulus are shown in Figure 2. The results show that the temperature difference between the superior surface and bottom surface of the ceramic plate approximately linear increases with the increment of slow heating rate and independent of minor frame Young's modulus. And the heating rate $0.1°C \cdot s^{-1}$ will be used to heating up from the predefined temperature field to thermal shock initial temperature in this paper.

4. Numerical Simulation for Thermal Shock Resistance under Temperature Rising

The critical temperature differences of rupture corresponding to the heating rate for various frame Young's modulus are shown in Figure 3. The results show that the critical

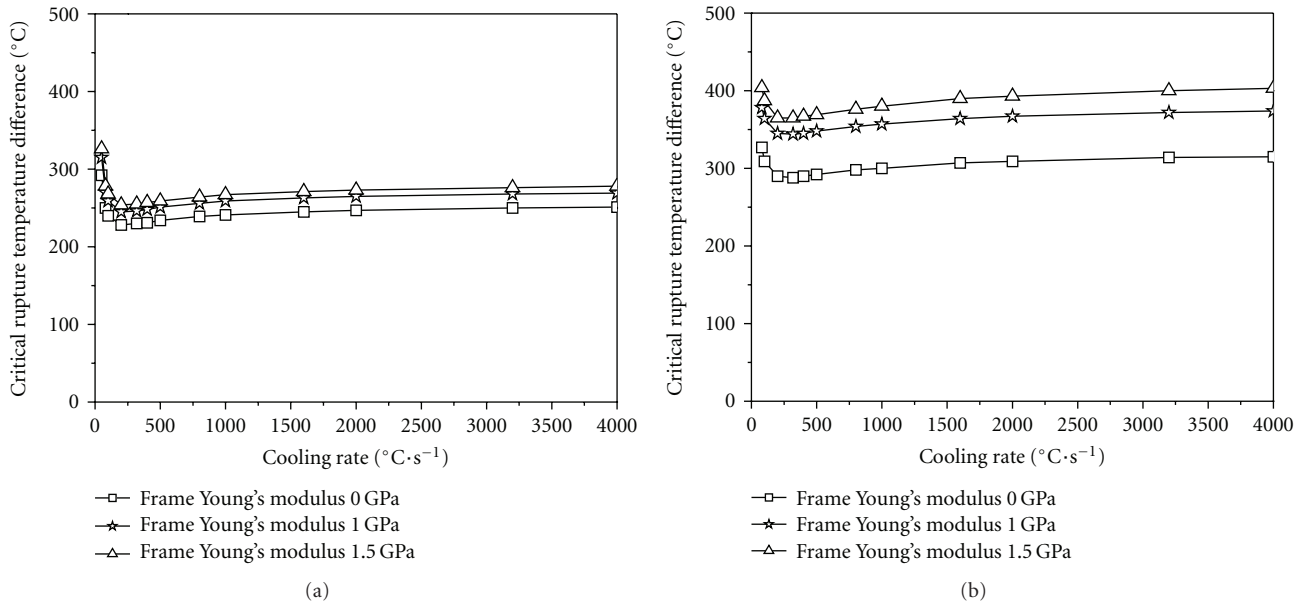

Figure 6: The critical rupture temperature difference versus cooling rate for different frame Young's modulus with the thermal shock initial temperature (a) 1500°C and (b) 1900°C.

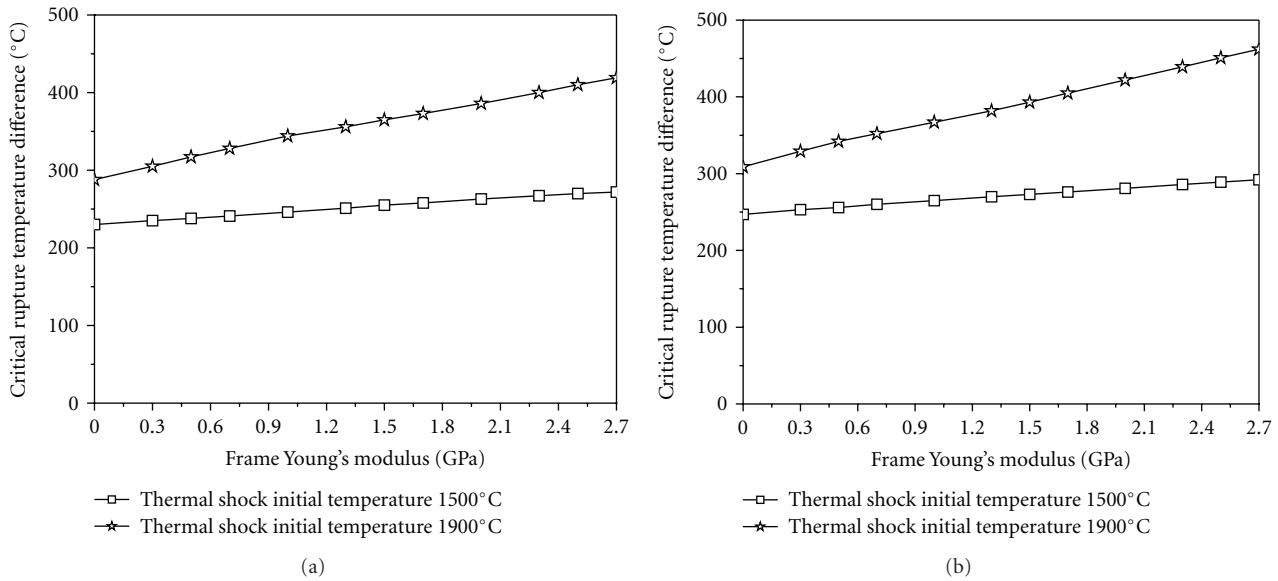

Figure 7: The critical rupture temperature difference versus frame Young's modulus for different thermal shock initial temperature with the same cooling rate (a) 320°C·s^{-1} and (b) 2000°C·s^{-1}.

rupture temperature differences of the ceramic plate firstly decrease sharply and then reach a minimum value, and afterwards increase gently as heating rate increases. A danger heating rate region exists near 300°C·s^{-1} where the critical temperature difference is the lowest. It is clear that the TSR of ceramic plate decreases with the strengthening of external constraint for the thermal shock of heating up, and the higher thermal shock initial temperatures the greater influence from the external constraint.

The critical temperature differences of rupture corresponding to the frame Young's modulus for various thermal shock initial temperatures are shown in Figure 4. The results show that the critical rupture temperature differences decrease approximately linearly with the increment of frame Young's modulus for heating up, and the higher thermal shock initial temperature the greater influence from the external constraint.

The critical temperature differences of rupture corresponding to the thermal shock initial temperature for various frame Young's modulus are shown in Figure 5. The results show that the critical temperature differences of the ceramic plate firstly decrease and then reach a minimum value and

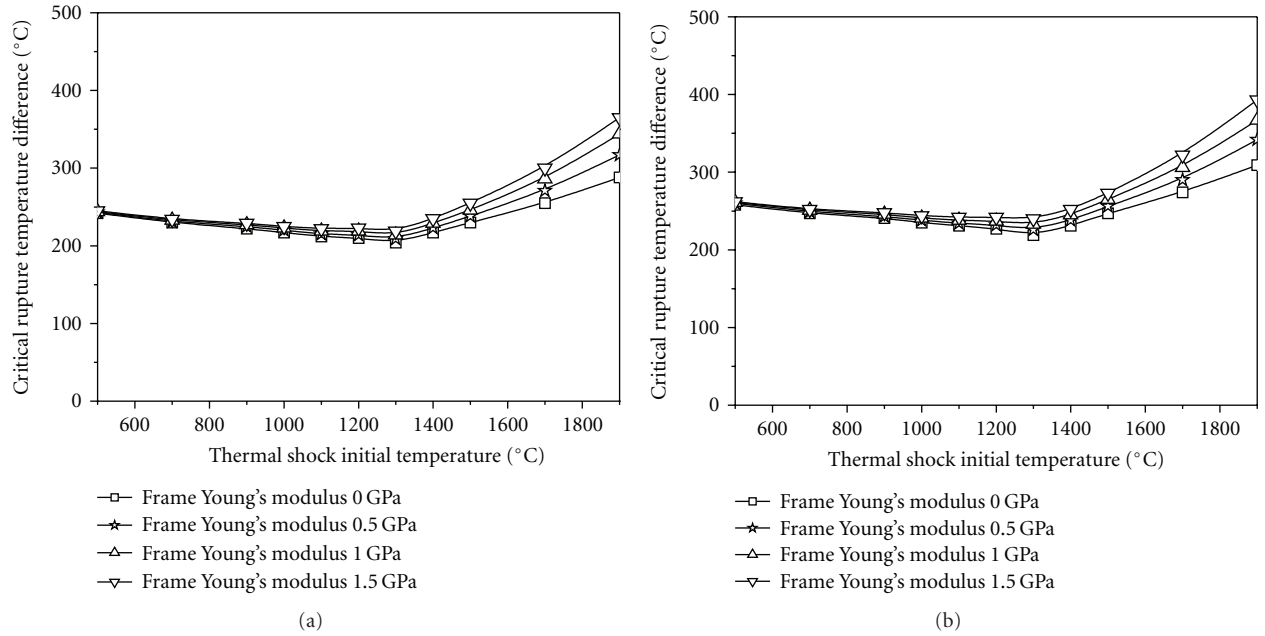

Figure 8: The critical rupture temperature difference versus thermal shock initial temperature for different frame Young's modulus with the same cooling rate (a) $320^{\circ}C \cdot s^{-1}$ and (b) $2000^{\circ}C \cdot s^{-1}$.

afterwards increase as thermal shock initial temperature increases. A danger thermal shock initial temperature region exists near 900°C where the critical temperature difference is lowest. It is clear that the TSR of the ceramic plate decreases with the strengthening of external constraint for the thermal shock of heating up, and the higher thermal shock initial temperature, the greater influence from the external constraint.

5. Numerical Simulation for Thermal Shock Resistance under Temperature Dropping

The effects of cooling rate, external constraint, and thermal shock initial temperature on the critical rupture temperature difference of ceramic plate for cool down have been presented in Figures 6, 7, and 8, respectively. Comparing with the case of the temperature rising, the similar results can be obtained. But the critical temperature differences of rupture increase with the strengthening of external constraint for the thermal shock of cool down. The external constraint prepares a compressive stress field in the structure because of the predefined temperature field, and this compressive stress field relieves the tension stress in the structure when it is cooled down and then the TSR of the UHTCs is improved. Besides a danger thermal shock initial temperature region exists near 1300°C where the critical temperature difference is lowest.

6. Conclusions

In this paper, the initial stress field was set up before thermal shock by slow heating from predefined temperature field to thermal shock initial temperature field. The initial stress field relieved the stress field caused by thermal shock under cooling down and aggravated the stress field caused by thermal shock under heating up. Thereupon, the thermal shock resistance was increased under cooling down and decreased under heating up. As the thermal shock initial temperature, a danger heating rate (or cooling rate) exists where the critical temperature difference is the lowest.

Acknowledgment

This work was supported by the National Natural Science Foundation of China under Grants nos. 90916009, 11172336, and 10702035.

References

[1] J. D. Bull, D. J. Rasky, and J. C. Karika, "Stability characterization of diboride composites under high velocity atmospheric flight conditions," *International SAMPE Electronics Conference*, vol. 24, no. 13, pp. 1092–1106, 1992.

[2] M. M. Opeka, I. G. Talmy, E. J. Wuchina, J. A. Zaykoski, and S. J. Causey, "Mechanical, thermal, and oxidation properties of refractory hafnium and zirconium compounds," *Journal of the European Ceramic Society*, vol. 19, no. 13-14, pp. 2405–2414, 1999.

[3] S. R. Levine, E. J. Opila, M. C. Halbig, J. D. Kiser, M. Singh, and J. A. Salem, "Evaluation of ultra-high temperature ceramics for aeropropulsion use," *Journal of the European Ceramic Society*, vol. 22, no. 14-15, pp. 2757–2767, 2002.

[4] F. Song, S. H. Meng, X. H. Xu, and Y. F. Shao, "Enhanced thermal shock resistance of ceramics through biomimetically inspired nanofins," *Physical Review Letters*, vol. 104, no. 12, Article ID 125502, 4 pages, 2010.

[5] W. D. Kingery, H. K. Bowen, and D. R. Uhlmann, *Introduction to Ceramics*, chapter 16, John Wiley & Sons, New York, NY, USA, 2nd edition, 1976.
[6] D. J. Green, *An Introduction to the Mechanical Properties of Ceramics*, chapter 9, Cambridge University Press, Cambridge, UK, 1998.
[7] M. Collin and D. Rowcliffe, "Analysis and prediction of thermal shock in brittle materials," *Acta Materialia*, vol. 48, no. 8, pp. 1655–1665, 2000.
[8] C. Aksel, "The effect of mullite on the mechanical properties and thermal shock behaviour of alumina-mullite refractory materials," *Ceramics International*, vol. 29, no. 2, pp. 183–188, 2003.
[9] Z. H. Jin and R. C. Batra, "Thermal shock cracking in a metal-particle-reinforced ceramic matrix composite," *Engineering Fracture Mechanics*, vol. 62, no. 4-5, pp. 339–350, 1999.
[10] Z. H. Zhou, P. D. Ding, S. H. Tan, and J. S. Lan, "A new thermal-shock-resistance model for ceramics: Establishment and validation," *Materials Science and Engineering A*, vol. 405, no. 1-2, pp. 272–276, 2005.
[11] W. G. Li and D. N. Fang, "Effects of thermal environments on the thermal shock resistance of ultra-high temperature ceramics," *Modern Physics Letters B*, vol. 22, no. 14, pp. 1375–1380, 2008.
[12] P. Pettersson, M. Johnsson, and Z. Shen, "Parameters for measuring the thermal shock of ceramic materials with an indentation-quench method," *Journal of the European Ceramic Society*, vol. 22, no. 11, pp. 1883–1889, 2002.
[13] X. H. Zhang, L. Xu, S. Y. Du, W. B. Han, J. C. Han, and C. Y. Liu, "Thermal shock behavior of SiC-whisker-reinforced diboride ultrahigh-temperature ceramics," *Scripta Materialia*, vol. 59, no. 1, pp. 55–58, 2008.
[14] Y. F. Shao, X. H. Xu, S. H. Meng, G. H. Bai, C. P. Jiang, and F. Song, "Crack patterns in ceramic plates after quenching," *Journal of the American Ceramic Society*, vol. 93, no. 10, pp. 3006–3008, 2010.
[15] S. H. Meng, F. Qi, H. B. Chen, Z. Wang, and G. H. Bai, "The repeated thermal shock behaviors of a ZrB_2-SiC composite heated by electric resistance method," *International Journal of Refractory Metals and Hard Materials*, vol. 29, no. 1, pp. 44–48, 2011.
[16] J. C. Han and B. L. Wang, "Thermal shock resistance of ceramics with temperature-dependent material properties at elevated temperature," *Acta Materialia*, vol. 59, pp. 1373–1382, 2011.
[17] W. G. Li, D. Y. Li, C. Wang, and D. N. Fang, "Numerical simulation for thermal shock resistance of thermal protection materials under temperature rising," *Advanced Materials Research*, vol. 197-198, pp. 1509–1514, 2011.
[18] O. Knacke and O. Kubaschewski, *Thermochemical Properties of Inorganic Substances*, Springer, Berlin, Germany, 2nd edition, 1991.
[19] W. G. Li, R. Z. Wang, D. Y. Li, and D. N. Fang, "A model of temperature-dependent Young's modulus for ultrahigh temperature ceramics," *Physics Research International*, vol. 2011, Article ID 791545, 3 pages, 2011.
[20] W. G. Li, F. Yang, and D. N. Fang, "The temperature-dependent fracture strength model for ultra-high temperature ceramics," *Acta Mechanica Sinica*, vol. 26, no. 2, pp. 235–239, 2010.